free-flight data and show a trend of increasing stability with decreasing Mach number.

3) The free-flight technique has been successfully used in a continuous-flow transonic wind tunnel and has important advantages compared to other free-flight techniques. Model characteristics may be optimized to emphasize the desired data under controlled initial conditions, angle of attack, roll, and yaw. These important advantages are supported by the large number of data points (approximately 300), defining model angular motion history and flowfield characteristics. It is suggested that a biplanar mirror system developed for use with a conventional wind tunnel[11] would extend the present planar capability to the study of nonplanar motion of spinning models. The comparison of planar and nonplanar motion under the same test conditions would then be practical.

4) The data presented herein were used in a six-degree-of-freedom computer simulation. No alarming motions, such as tumbling or even large amplitude of oscillation, were observed, even when the hypothesized vehicle experienced a gust-induced angle of attack of 11° at $M = 2$ and 97,000-ft altitude.

References

[1] Dayman, B., Jr., "Free-Flight Testing in High-Speed Wind Tunnels," AGARDograph 113, NATO-AGARD, Paris, May 1966.

[2] Holway, H., Herrera, G., and Dayman, B., Jr., "A Pneumatic Model Launcher for Free-Flight Testing in a Conventional Wind Tunnel," TM 33-177, July 30, 1964, Jet Propulsion Lab., Pasadena, Calif.

[3] Prislin, R. H., "Free-Flight and Free-Oscillation Techniques for Wind Tunnel Dynamic Stability Testing," TR 32-878, March 1966, Jet Propulsion Lab., Pasadena, Calif.

[4] Marko, W. J., "Static Aerodynamic Characteristic of Three Blunted Sixty-Degree Half-Angle Cones at Mach Numbers from 0.60 to 1.30," TR 32-1298, July 1968, Jet Propulsion Lab., Pasadena, Calif.

[5] Walker, B. and Weaver, R. W., "Static Aerodynamic Characteristics of Blunted Cones in the Mach Number Range from 2.2 to 9.5," TR 32-1213, Dec. 1967, Jet Propulsion Lab., Pasadena, Calif.

[6] Marko, W. J., "Transonic Dynamic and Static Stability Characteristics of Three Blunt Cone Planetary Entry Shapes," TR 32-1357, July 1969, Jet Propulsion Lab., Pasadena, Calif.

[7] Krumins, M. V., "Drag and Stability of Mars Probe/Lander Shapes," *Journal of Spacecraft and Rockets*, Vol. 4, No. 8, Aug., 1967, pp. 1052–1057.

[8] Whitlock, C. H. and Bendura, R. J., "Dynamic Stability of a 4.6-Meter-Diameter 120-deg Conical Spacecraft at Mach Numbers from 0.78 to 0.48 in a Simulated Martian Environment," TND-4858, May 1968, NASA.

[9] Bendura, R. J., "Low Subsonic Static and Dynamic Stability Characteristics of Two Blunt 120-Deg Cone Configurations," TND-3853, 1967, NASA.

[10] Jaffe, P., "A Generalized Approach to Dynamic-Stability Flight Analysis," TR 32-757, July 1965, Jet Propulsion Lab., Pasadena, Calif.

[11] Prislin, R. H. and Holway, H. P., "A Wind Tunnel Free-Flight Testing Technique for Nonplanar Motion of Spinning Models," AIAA Paper 66-774, Los Angeles, Calif., 1966.

DECEMBER 1969 J. SPACECRAFT VOL. 6, NO. 12

Characteristics of Atmospheric Turbulence as Related to Wind Loads on Tall Structures

GEORGE H. FICHTL,* JOHN W. KAUFMAN,† AND WILLIAM W. VAUGHAN‡

NASA Marshall Space Flight Center, Ala.

An engineering boundary-layer wind model based on data collected at the NASA 150-m meteorological tower facility at the Kennedy Space Center, Fla. is presented. Hourly peak-wind profiles of the form $u(z) = u_{18}(z/18)^k$ and climatological hourly peak-wind statistics at the 10-m level are used to specify design peak-wind profiles, where $u(z)$ is the hourly peak wind speed at height z in meters, u_{18} is the 18-m level peak-wind speed, and $k = bu_{18}^{-3/4}$. The parameter b is normally distributed. The relationship between the instantaneous extreme and the peak-wind profiles for time periods up to ten minutes is examined. The use of the peak-wind profile concept in design studies could produce overestimates in drag loads. Empirical formulas are obtained to estimate the gust factor $G(z) = u(z)/\bar{u}(z)$, where $\bar{u}(z)$ is the time mean wind at height z associated with a specified averaging time. The gust factor is a monotonically increasing function of the averaging time and a decreasing function of z. For daytime conditions the gust factor is a monotonically decreasing function of u_{18}, while for nighttime conditions, it is a monotonically increasing function of u_{18}. A spectral model of the longitudinal and lateral components of turbulence for the neutral boundary layer (high-wind speeds) is presented. The model accounts for the vertical variation of turbulence power spectra.

Nomenclature

b = parameter that characterizes the statistics of k
C_p = specific heat of dry air at constant pressure
C = empirically determined parameter that occurs in formulas of the longitudinal and lateral spectra
f = $nz/\bar{u}$
f_m = value of f associated with peak of logarithmic spectrum

Received March 28, 1969; revision received August 20, 1969. The authors wish to thank Mr. O. E. Smith for his interest, helpful comments, discussion, and use of Fig. 1.

* Scientific Assistant.

† Chief, Atmospheric Dynamics Branch.

‡ Chief, Aerospace Environment Division, Aero-Astrodynamics Laboratory. Associate Fellow AIAA.

g = acceleration of gravity
g_0 = empirical function of u_{18} and t that occurs in the formulas for the gust factor
G = gust factor
k = peak wind profile parameter
k_1 = 0.4 = von Kármán's constant
L' = stability length
n = frequency, Hz
p = empirical function of u_{18} that occurs in the formulas for the gust factor
r = empirically determined parameter that occurs in formulas of the longitudinal and lateral spectra
Ri = gradient Richardson number
$S(n)$ = longitudinal or lateral spectrum of turbulence
t = averaging time
$\bar{T}$ = time average mean temperature
$u(z)$ = peak wind speed at height z
$\bar{u}(z)$ = time averaged mean wind speed at height z
u_{*0} = surface friction velocity
z_0 = surface roughness length
β = vertical collapsing factor
σ = standard deviation of k
σ_t = standard deviation of the turbulence associated with frequencies greater than approximately $1/2t$ (Hz)
ψ = logarithmic wind profile stability defect.

Introduction

THE purpose of ground wind criteria is to provide a model of the atmospheric boundary layer such that when it is used in design studies an acceptable structure results. How such a model should be developed is determined by the purpose and requirements of the structure. This paper presents a ground-wind model suitable for the design of space vehicles and related tall structures. Although the model is valid only for the Kennedy Space Center, the ideas and principles used to develop it can be applied to other launch or building sites.

Peak Wind Statistics

The fundamental ground wind statistics for the Kennedy Space Center are based on an eight-year sample of hourly peak-wind speeds measured at the 10-m level for a period of record from Sept. 1958 through June 1967. The sample was constructed for NASA by the National Weather Records Center, Asheville, N. C., by selecting the peak-wind speed that occurred in each hour of record read from original wind rolls. Peak-wind statistics do not depend on an averaging operation as do mean-wind estimates, and in this respect, peak-wind statistics are more fundamental.

Smith et al.[1] have performed extensive statistical analyses with the Kennedy Space Center peak-wind speed sample and have introduced the concept of exposure period probabilities into the design and operation of space vehicles. By determining the distribution functions of peak-wind speeds for various periods of exposure (hour, day, month, year, etc.), it is possible to determine the probability that a certain peak-wind-speed magnitude will occur during a prescribed period of exposure of a space vehicle to the natural environment. Thus, for example, if an operation requires, say, one hour to complete, and if the critical wind loads on the vehicle can be defined in terms of the peak-wind speed, then it is the probability of occurrence of the peak wind speed during a one-hour period that gives a measure of the probable risk of the occurrence of structural failure. Similarly, if an operation requires one day to complete, then it is the probability of occurrence of the peak wind during a one-day period that gives a measure of the probable risk of structural failure.

Smith et al.[1] have shown that the peak-wind speeds at Cape Kennedy for various periods of exposure can be statistically represented with a Fisher-Tippett Type I distribution[2] which is the one used by Gumbel.[3] Although the Gumbel distribution seems to give a good theoretical fit to the empirical peak-wind speed distribution, it has the disadvantage that it is unbounded at both ends. Since wind speed has a physical lower bound at zero, it may be desirable in the future to investigate other distribution functions. Smith points out that the Fisher-Tippett Type II distribution, which is indeed bounded from below at zero, would be such a function. Thom[4] has used the Fisher-Tippett Type II distribution for representing ground wind statistics.

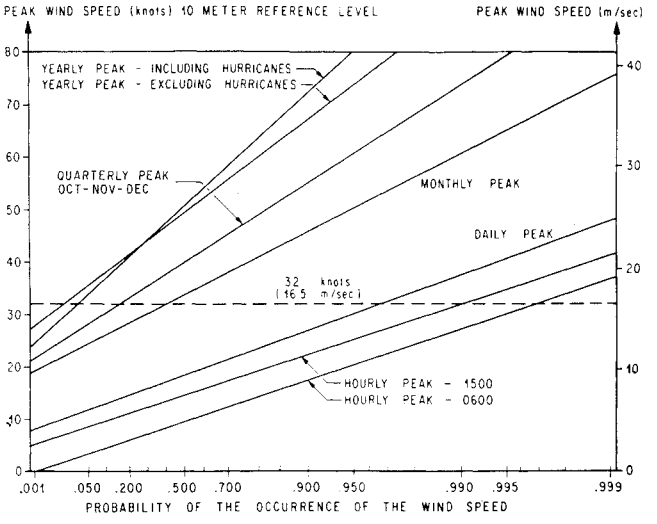

Fig. 1 Fisher-Tippett type I or Gumbel distributions of the daily, hourly (0600 and 1500 EST), and monthly peak wind speeds for Oct. at Cape Kennedy, Fla. Included in the figure are the quarterly (Oct.-Nov.-Dec.) and the yearly (excluding and including hurricanes) peak wind speed distributions.

Figure 1 shows an example of Smith's peak-wind speed distributions, for the month of October for different reference periods, from which the probabilities of the occurrences of peak-wind speeds for the indicated reference periods can be determined. Thus, for example, the probability that the peak-wind speed during the hour from 0530 to 0630 EST (0600 EST) will be less than 32 knots is approximately 0.997.

Probability statements concerning the capabilities of the space vehicles developed at the Marshall Space Flight Center and launched at the Kennedy Space Center are given in terms of Smith's peak-wind speed exposure statistics, which are valid at the 10-m level. However, to perform loading and response calculations resulting from steady-state and random turbulent drag loads and von Kármán vortex shedding loads, the engineer requires information about the vertical variation of the mean-wind speed and the structure of turbulence in the atmospheric boundary layer. The procedure is to extrapolate the peak-wind statistics upward into the atmosphere with a statistical peak-wind profile model and to obtain the associated quasi-steady or mean-wind speed profile by dividing the peak-wind speed with a gust factor, which is a function of wind, speed, and height. The gust factor is equal to the peak-wind speed divided by a mean-wind speed obtained by averaging the wind-speed-time history over a particular interval of time, which is usually less than one hour. At this point, the engineer can calculate the steady-state loads resulting from the mean-wind profile and the response due to discrete gusts. The gust factor accounts for the loads beyond these resulting from the quasi-steady or mean-wind profile—in short, the turbulence. In the strictest sense, fluid flows which qualify as turbulence must be rotational, dissipative, three-dimensional, nonlinear, stochastic, and diffusive. We define turbulence to be the velocity fluctuations about the mean-wind profile velocity. For some applications, depending on the response characteristics of the vehicle, the peak-wind speed profile is used directly in the calculations. An alternative, and probably more meaningful, representation of the turbulence can be

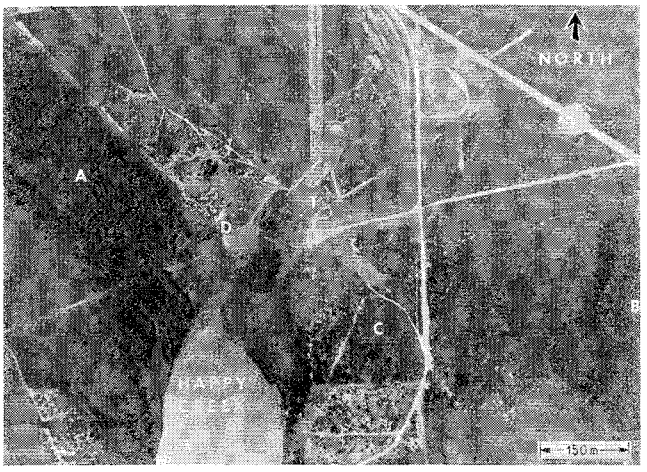

Fig. 2 Aerial plan view of the terrain surrounding the NASA 150-m meteorological tower.

given in the form of a spectral model of the longitudinal and lateral components of turbulence.

NASA 150-m Meteorological Tower

To obtain micrometeorological data representative of the Kennedy Space Center area, a 150-m meteorological tower was constructed on Merritt Island approximately 5 km from the Saturn V launch pads in launch complex 39. Located about 4.5 km from the Atlantic Ocean, the tower is situated in a well-exposed area free of near-by structures which could interfere with the airflow. The tower facility, discussed in a more detailed report by Kaufman and Keene,[5] is only briefly described here.

The tower is instrumented at the 18-m, 30-m, 60-m, 90-m, 210-m, and 150-m levels with Climet (Model Cl-14) wind sensors. Temperature sensors, Climet (Model-016) aspirated thermocouples are located at the 18-m, 30-m, 60-m, 120-m, and 150-m levels.

The aerial photograph (Fig. 2) of the terrain surrounding the tower (point T) was taken at approximately 1200 m above mean sea level. In the quadrant from an azimuth of approximately 300° north with respect to the tower, clockwise around to 90°, the terrain is homogeneous, being covered with vegetation about one-half to 2 m high. Another homogeneous area with the same type of vegetation occurs in the 135° to 160° quadrant. The areas A (230°–300°), B (90°–135°), and C (160°–180°) are covered with trees from about 10 to 15 m tall. The fetch from the tower to areas A or C is about 200 m, and the fetch to area B is about 450 m. The height of the vegetation over these fetches varies from $\frac{1}{2}$ to $1\frac{1}{2}$ m, as in the area to the north of the tower. To the south-southwest in the 180° to 230° quadrant 225 m from the tower, there is a body of water called Happy Creek.

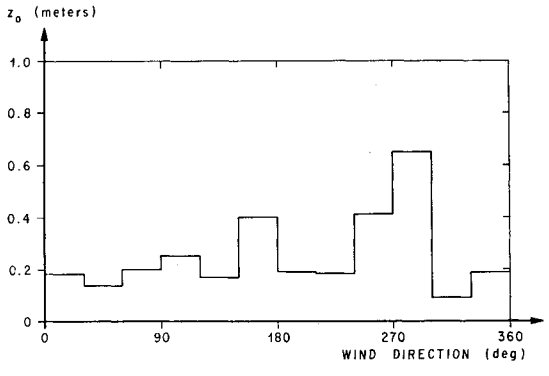

Fig. 3 Distribution of the surface roughness length at the NASA 150-m meteorological tower site.

Fichtl[6] and Fichtl and McVehil[7] have calculated the surface roughness length configuration associated with the NASA tower. The surface roughness length is the height below which the mean wind vanishes and the flow is completely turbulent. The analysis was based on wind profile laws that are consistent with the Monin-Obukhov similarity hypothesis and turbulent energy budget considerations at the 18-m level. The results of these calculations, shown in Fig. 3, show the effects of the terrain features on the surface roughness.

Design Wind Profiles

To calculate wind loads on space vehicles, the engineer requires specific information about the peak and mean-wind profiles. In this section, we present a statistical wind profile model and gust factor model suitable for this purpose. All ground wind speed statements should include the associated reference height due to variation of wind speed in the vertical.

Peak-Wind Profiles

To develop a peak-wind profile model, about 6000 hourly peak-wind speed profiles measured during the year 1967 were analyzed. The sample was constructed by selecting the peak-wind speed at each level for each hour of record. The data seemed to show that the variation of the hourly peak-wind speed in the vertical, below 150 m, could be described with a power law relationship given by

$$u(z) = u_{18}(z/18)^k \tag{1}$$

where $u(z)$ is the peak wind speed at height z above natural grade and u_{18} is a known peak-wind speed at $z = 18$ m. The parameter k was determined for each profile by a least-square analysis of the data.

At low wind speeds on the order of 2 msec^{-1}, the quantity k varied from about -0.15 to 0.9. Negative values of k occurred for approximately 8% of the cases in the sample. It should be kept in mind that we are analyzing peak-wind profiles and that it is possible for the peak-wind speed at some or all of the levels above 18 m to be less than the 18-m level peak-wind speed resulting in negative values of k. This is not to

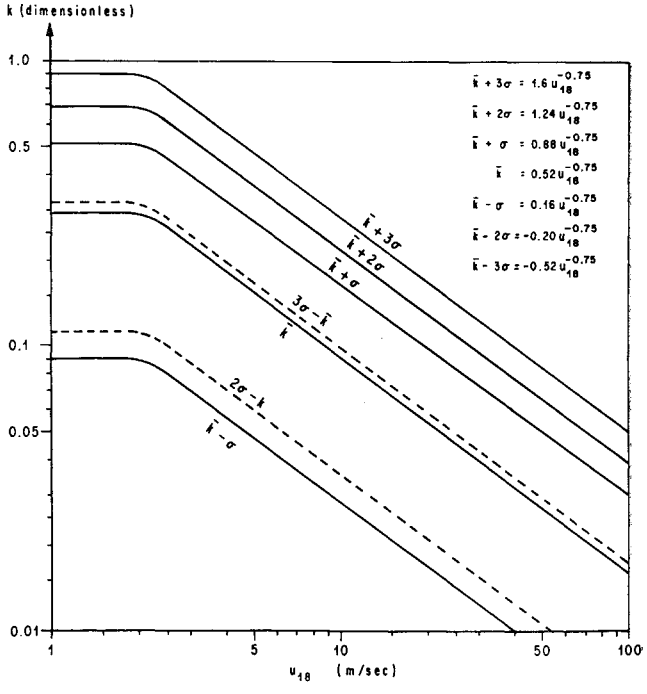

Fig. 4 The mean, $\pm\sigma$, $\pm2\sigma$, and $\pm3\sigma$ values of k as functions of the peak wind speed u_{18} at the 18-m level. The dashed curves correspond to negative values of k.

imply that the associated mean-wind speeds decrease in the vertical.

A statistical analysis of the data revealed that, for engineering purposes, k is distributed normally for any particular value of the peak wind speed at the 18-m level. Thus, for a given percentile level of occurrence, it was found that, for the 18-m level peak wind speeds less than approximately 2 msec^{-1}, k is equal to a constant, while for peak wind speeds greater than 2 msec^{-1},

$$k = bu_{18}^{-3/4} \tag{2}$$

where b is a parameter that is distributed normally with mean value $\bar{k}$ and standard deviation σ equal to 0.52 and 0.36 and u_{18} is in meters per second. The distribution of k as a function of u_{18} is shown in Fig. 4.

To apply (1) and (2) to the peak-wind statistics valid at 10 m, (1) is evaluated at $z = 10$ m, and it is asumed that the resulting relationship can be inverted to yield u_{18} as a function of the 10-m level peak wind speed u_{10} for a fixed value of b. This function is then combined with (2) to yield k as a function of u_{10} for a given value of b. The validity of this inversion process is open to question because (1) is a stochastic relationship. However, preliminary analyses of profiles that include peak wind information obtained at the 10-m level seem to show that this inversion is valid.

The current design practice at the Marshall Space Flight Center is to use the $\bar{k} + 3\sigma$ value of k to determine operational limits for space vehicles. Thus, if a space vehicle designed to withstand a particular value of the peak-wind speed at the 10-m level is exposed to that peak-wind speed, the vehicle has at least a 99.87% chance of withstanding the associated smoothed peak wind speed profile.

Instantaneous Extreme Wind Profiles

Because the probability that the hourly peak-wind speeds at all levels occur simultaneously is small, the practice of using peak-wind profiles introduces some conservatism into design criteria. In this section we estimate the amount of conservatism involved.

To gain some insight into this question, about 35 hr of digitized magnetic tape data were analyzed. The data were digitized at 0.1-sec intervals in real time and partitioned into 0.5-, 2-, 5-, and 10-min samples. The vertical-average, horizontal peak-wind speed $\bar{u}_p$ and the 18-m time mean-wind $\bar{u}_{18}$ were calculated for each sample. In addition, the instantaneous vertical-average, horizontal wind speed time history at 0.1-sec intervals was calculated for each sample, and the maximum instantaneous vertical-average, horizontal wind speed $\bar{u}_I$ was selected from each sample. The quantity $\bar{u}_I/\bar{u}_p$ was then interpreted to be a measure of how well the peak-wind profile statistics at the 10-m level approximate instantaneous extreme wind profile statistics.

In Fig. 5, a plot of $\bar{u}_I/\bar{u}_p$ as a function of $\bar{u}_{18}$ for a 10-min averaging period, the data points tend to scatter about a mean value of $\bar{u}_I/\bar{u}_p \simeq 0.93$. Since drag loads are proportional to the square of the velocity, this result implies that the peak-wind profile could produce overestimates in drag loads by about 14%. However, some of the data points have values equal

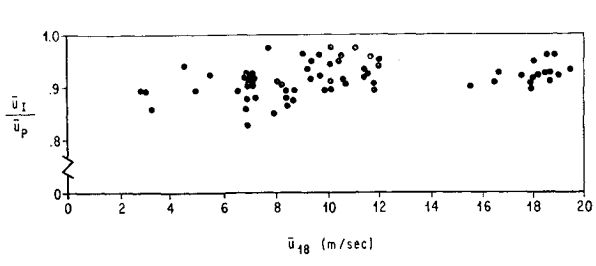

Fig. 5 The ratio $\bar{u}_I/\bar{u}_p$ as a function of the mean wind speed $\bar{u}_{18}$ at the 18-m level for an averaging time equal to 10 min.

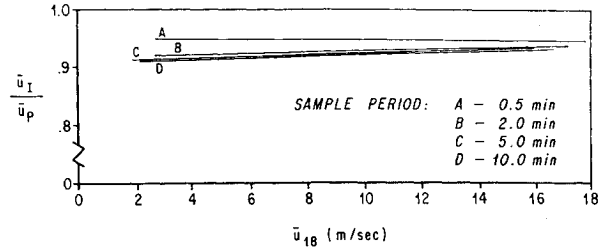

Fig. 6 The ratio $\bar{u}_I/\bar{u}_p$ as a function of the mean wind speed $\bar{u}_{18}$ at the 18-m level for various averaging times.

to 0.98 which might correspond to an over-estimate of the loads by only 4%. Figure 6 shows the average values of $\bar{u}_I/\bar{u}_p$ as a function of $\bar{u}_{18}$ for different averaging times (0.5, 2, 5, and 10 min).

Gust Factor

The gust factor G is defined as

$$G = u/\bar{u} \tag{3}$$

where u is the peak-wind speed within a data record of length t in time, and $\bar{u}$ is the mean-wind speed associated with the data record. The gust factor is used to transform peak-wind speeds to mean-wind speeds. A simple theory can be constructed to aid in understanding the behavior of the gust factor. If σ_t denotes the standard deviation of the longitudinal fluctuations of the velocity about the mean-wind speed associated with an averaging time t, then $\bar{u} + 3\sigma_t$ is an estimate of the peak-wind speed in the time interval t; therefore,

$$G = 1 + 3\sigma_t/\bar{u} \tag{4}$$

The standard deviation of the turbulence can be related to the wind profile through the surface friction velocity u_{*0}, which is the square root of the tangential stress per unit mass at the surface of the earth. In approximately the first 30 m of the boundary-layer longitudinal and lateral turbulence spectra can be represented as

$$nS(n)/u_{*0}^2 = F(f,Ri) \tag{5}$$

if it is assumed that the similarity theory of Monin[8] for the vertical velocity spectrum can be applied to the longitudinal and lateral spectra. In this equation, $S(n)$ is spectrum of the longitudinal or lateral components of turbulence associated with frequency n(Hz) and integration of $S(n)$ over the domain, $0 < n < \infty$, will yield the variance of the longitudinal or lateral components of turbulence. In the Monin layer ($z < 30$ m) the function $F(f,Ri)$ is a universal function of the dimensionless wave number f and the Richardson number Ri, which are given by

$$f = nz/\bar{u}(z) \tag{6}$$

and

$$Ri = \frac{(g/T)(g/C_p + \partial\bar{T}/\partial z)}{(\partial\bar{u}/\partial z)^2} \tag{7}$$

where $\bar{T}$ and $\bar{u}$ denote the mean Kelvin temperature and wind speed at height z, g is the acceleration of gravity, and C_p is the specific heat of dry air at constant pressure ($g/C_p = 9.8°$K/km). The Richardson number is a measure of the stability of the boundary layer. If $Ri > 0$, the boundary layer is statically stable while $Ri < 0$ corresponds to a statically unstable boundary layer. In the special case $Ri = 0$, we have a statically neutral boundary layer. The process of averaging the wind-speed time history over a period of time t corresponds to a low pass filter which removes the Fourier components with frequencies greater than approximately $1/2t$ (Hz) from the turbulence record. An estimate of σ_t can be obtained by

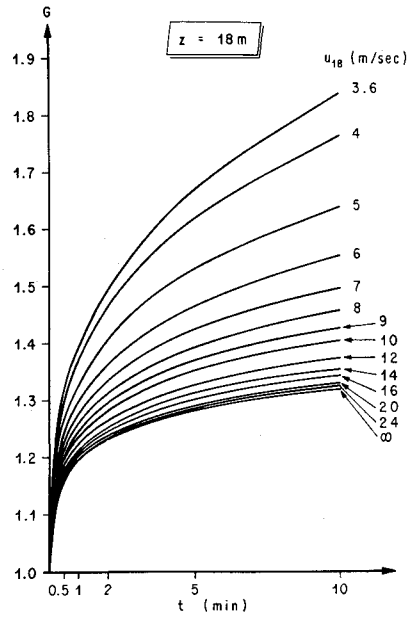

Fig. 7 The gust factor G at the 18-m level as a function of the averaging time for various peak wind speeds at the 18-m level.

integrating $S(n)$ over the interval $1/2t < n < \infty$, so that from (5) we conclude that

$$\sigma_t = A(Ri,t)u_{*0} \tag{8}$$

In this equation, $A(Ri,t)$ is a dimensionless function given by

$$A(Ri,t) = \left\{\int_{f_0}^{\infty} \frac{F(f,Ri)}{f}\, df\right\}^{1/2} \tag{9}$$

where $f_0 = z/2t\bar{u}(z)$. The function $F(f,Ri)/f$ is positive definite so that $A(Ri,t)$, and thus σ_t are monotonically increasing functions of the averaging time t.

According to Lumley and Panofsky[9] the mean-wind profile in approximately the first 30 m of the atmosphere is given by

$$\bar{u} = (u_{*0}/k_1)[\ln(z/z_0) - \psi(Ri)] \tag{10}$$

where k_1 is von Kármán's constant with a numerical value approximately equal to 0.4, and z_0 is the surface roughness length. The quantity $\psi(Ri)$ is a universal function of Ri and is given by

$$\psi(Ri) = 0.044\left(\frac{-Ri/0.01}{(1-18Ri)^{1/4}}\right)^{1.0674-0.678\ln[(-Ri/0.01)/(1-18Ri)^{1/4}]} \qquad (Ri < -0.01) \tag{11}$$

$$\psi(Ri) = -4.5Ri \qquad (-0.01 \leqq Ri \leqq 0.01) \tag{12}$$

$$\psi(Ri) = -7Ri/(1-7Ri) \qquad (0.01 < Ri \leqq 0.1) \tag{13}$$

Eq. (11) is a least-squares representation of $\psi(Ri)$ which is given graphically by Lumley and Panofsky.[9] The forms of $\psi(Ri)$ given by (12) and (13) were suggested by Panofsky, Blackadar, and McVehil.[10]

Upon combining (3), (4), (8), and (10), we find that

$$G = 1 + 3k_1A(Ri,t)/[\ln(z/z_0) - \psi(Ri)] \tag{14}$$

For a neutral atmosphere, $Ri = 0$, and ψ vanishes, so that

$$G = 1 + \frac{3k_1A(0,t)}{\ln(z/z_0)} \tag{15}$$

We may conclude from this relationship that the gust factor decreases as the height increases. This result is also qualitatively true for unstable air ($Ri < 0$). As the averaging time decreases, A decreases, and thus we may conclude from (14) that G is an increasing function of the averaging time. It should be noted that (14) predicts that the gust factor is a monotonically increasing function of the roughness z_0.

The functions ψ and A are monotonically decreasing functions of the Richardson number; ψ vanishes in neutral ($Ri = 0$) air, while A is positive definite. Thus, as the Richardson number decreases, or rather, as the air becomes more unstable, the gust factor increases.

Let us now consider a typical daytime situation at the Kennedy Space Center. At low wind speeds, the air is unstable and G is large. However, as the wind speed increases, the mean wind shear ($\partial\bar{u}/\partial z$) increases and because of turbulent mixing $\partial\bar{T}/\partial z$ approaches $-g/C_p$, causing the Richardson number to tend to zero from the unstable side of $Ri = 0$. Thus, an increase in the wind speed will tend to lower the gust factor, because of the dependence of the gust factor upon stability. In a typical nighttime situation, the stratification is stable, and the Richardson number is positive. As the wind speed increases, the Richardson number tends to zero from the stable side of $Ri = 0$. This means that the gust factor will tend to increase as the wind speed increases. In both cases the limiting value of the gust factor will be that of a neutral atmosphere ($Ri = 0$) as given by (15). Equation (14) is valid for $z < 30$ m; however, the conclusions that were obtained from this equation qualitatively hold for heights greater than 30 m.

In view of these considerations, a gust factor model for the Kennedy Space Center was developed with 181 hr of afternoon turbulence data encompassing a broad range of wind speed conditions. Gust factors were calculated for averaging times equal to 0.5, 1, 2, 5, 10, and 60 min. It was assumed that the gust factor is a function of both the averaging time and the peak wind speed u_{18} at the 18-m level, the latter playing the role of a stability parameter. It was found that the expected value of the gust factor at any level between 18 and 150 m can be represented as

$$G = 1 + (1/g_0)(18/z)^p \tag{16}$$

where z is the height in meters. In this equation, the parameters p and g_0 are given by

$$p = 0.283 - 0.435e^{-0.2u_{18}} \tag{17}$$

and

$$g_0 = 1.98 + 0.085[\ln(t/10)]^2 - 0.329\ln(t/10) - 1.887e^{-0.2u_{18}} \tag{18}$$

where t and u_{18} have the units of minutes and meters per second. The dependence of the 18-m level gust factor on the averaging time and the peak wind speed is shown in Fig. 7,

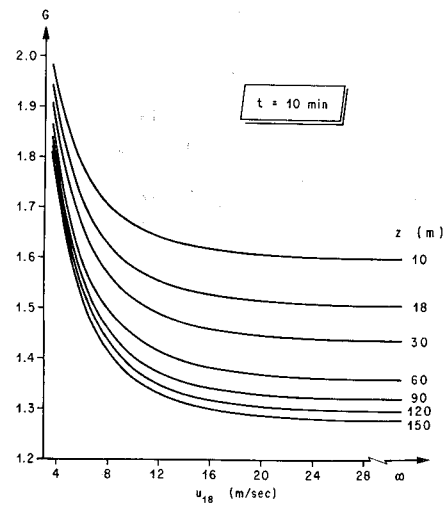

Fig. 8 The gust factor G as a function of the peak wind at the 18-m level for various heights above natural grade and a 10-min grand average.

and the dependence of the 10-m gust factor on the peak wind speed and height is shown in Fig. 8.

Within the range of variation of the data, the 1-hr gust factor and the 10-m gust factor were approximately equal, because the spectrum of the horizontal wind speed near the ground is characterized by a broad energy gap centered at a frequency approximately equal to 1 cycle hr^{-1} and typically extends over the frequency domain 0.5 cycles $hr^{-1} < n < 5$ cycles hr^{-1} (see Ref. 9). The spectral components associated with frequencies less than 1 cycle hr^{-1} correspond to the mesoscale and synoptic scale motions, while the remaining high-frequency spectral components correspond to mechanically and thermally produced turbulence. Thus, a statistically stable estimate of the mean or steady-state wind speed can be obtained by averaging over a period in the range from 10 min to an hour. Davenport[11] points out that this averaging period is also suitable for structure analysis and since this period is far longer than any natural period of structural vibration, it assures that effects caused by the mean wind properly represent steady-state, nontransient effects.

Design Spectral Models

In many types of space vehicle response calculations, engineers have used the Fourier transform to solve the equations of motion which describe and predict the ultimate response of the space vehicle to the natural environment. Thus, the input function which describes the turbulent character of the drag loads must be specified in terms of Fourier amplitudes.

To establish a spectral model of turbulence for the Kennedy Space Center, approximately fifty cases of turbulence were analyzed. The procedure used to calculate the longitudinal and lateral components of turbulence consisted of 1) converting the digitized wind speeds and directions (10 data points/sec) into the associated north-south and east-west components and averaging these components over the duration time of each test, 2) calculating the mean wind speed and direction with the averaged components, 3) projecting the original digitized data onto the mean wind vector and subtracting the mean wind speed to yield the longitudinal components of turbulence, and 4) projecting the original digitized data onto a normal-to-the-mean-wind vector to obtain the lateral components of turbulence. Trends contained within the data were removed by fitting the longitudinal and lateral components of turbulence to second order polynomials and in turn subtracting these polynomials from the component time histories. To reduce computation time, the data, with trend removed, were block-averaged over half-second intervals. The longitudinal and lateral spectra were calculated by using the standard correlation Fourier transform methods given by Blackman and Tukey.[12] These spectra were corrected for the half-second block-averaging operation with the procedure given by Pasquill[13] and for the response properties of the instrumentation.

To combine the spectra for each level on the tower, it was assumed that they could be scaled according to the similarity

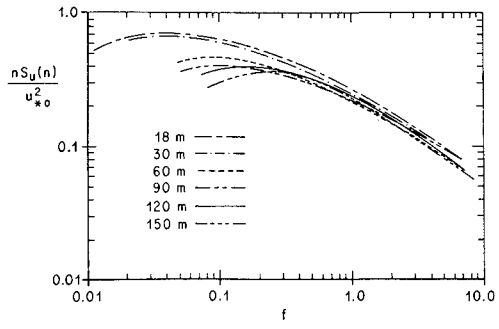

Fig. 9 Dimensionless logarithmic longitudinal spectra for neutral wind conditions plotted in Monin coordinates.

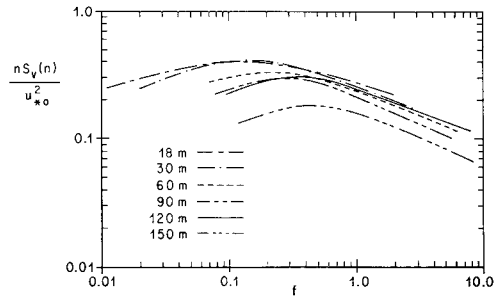

Fig. 10 Dimensionless logarithmic lateral spectra for neutral wind conditions plotted in Monin coordinates.

hypothesis of Monin[8] which is functionally represented by (5). The function F is tentatively a universal function of the dimensionless wave number f and the gradient Richardson number Ri.

The calculation of u_{*0} was based upon the wind data measured at the 18- and 30-m levels and the temperature data measured at the 18- and 60-m levels and the wind profile (10). Temperatures at the 30-m level were estimated by logarithmically interpolating between the 18- and 60-m levels. The gradient Richardson number, (7), at the 23-m level (geometric mean height between the 18- and 30-m levels) was estimated by assuming that the mean-wind speed and temperature are logarithmically distributed between these levels.

The meteorological conditions of particular inrerest are those associated with mean-wind speeds at the 18-m level which are greater than approximately 10 $msec^{-1}$. During these flow conditions, the boundary layer is well mixed so that vertical gradients of the mean flow entropy are small ($d\bar{T}/dz \simeq -g/C_p$) and the wind shears are large; thus, the Richardson number vanishes or at least becomes very small. Accordingly, the neutral longitudinal and lateral spectra are of particular interest in the design and operation of space vehicles. The neutral spectra were determined by extrapolating the data to $Ri = 0$ by the procedure developed by Berman.[14] Scaled spectra $nS(n)/u_{*0}^2$ were plotted against Ri for various values of f, and curves were drawn by eye. The values of $nS(n)/u_{*0}^2$ at $Ri = 0$ were then read off to yield the neutral spectra for the various levels on the tower. The results of this graphical process are shown in Figs. 9 and 10.

In Figs. 9 and 10, the position of the maxima shift toward higher values of f as the height increases. This means that Monin coordinates $(nS(n)/u_{*0}^2, f)$ fail to collapse the spectra in the vertical so that $F(f,Ri)$ is not a universal function, and thus an added height dependence should be included in the analysis. Busch and Panofsky[15] have obtained similar results from analyses of tower data from Round Hill.

To produce a vertical collapse of the data, it was assumed, for engineering purposes, that the spectra in Monin coordinates are shape-invariant in the vertical. This hypothesis appears to be reasonable and permits a practical approach to developing an engineering spectral model of atmospheric turbulence.

The Longitudinal Spectrum

The vertical variation of the dimensionless wave number f_{mu} associated with the peak of the logarithmic spectrum S_u scaled in Monin coordinates is shown in Fig. 11. A least-squares analysis of the data in this figure yields the result

$$f_{mu} = 0.03(z/18) \tag{19}$$

where z is in meters. A plot of $nS_u(n)/u_{*0}^2$ vs f/f_{mu} will shift the spectra at the various levels, so that all the peaks of the logarithmic longitudinal spectra are located at $f/f_{mu} = 1$. Values of f_{mu} from other tower sites are shown in Fig. 11.

The average ratio β_u of the shifted spectrum at level z and the 18-m spectrum $[S_u(f/f_{mu},z)/S_u(f/f_{mu},18)]$ is shown in Fig.

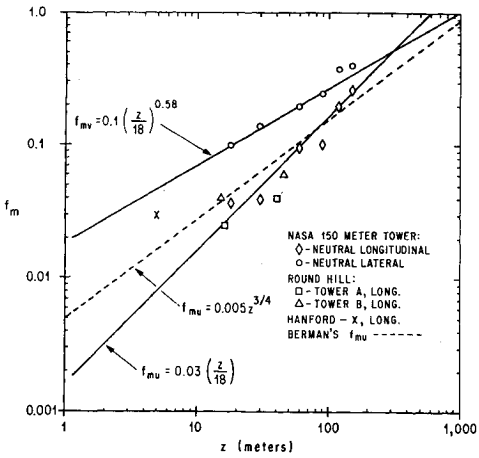

Fig. 11 Vertical distributions of the dimensionless frequencies f_{mu} and f_{mv} associated with the peak of the logarithmic longitudinal and lateral spectra for neutral stability conditions.

12. A least-squares analysis of these data yielded the result

$$\beta_u = (z/18)^{-0.63} \tag{20}$$

where z is in meters. A plot of $nS_u(n)/\beta_u u_{*0}^2$ vs f/f_{mu} will collapse the longitudinal spectra. The collapsed longitudinal data are plotted as a function of $0.03\,f/f_{mu}$ in Fig. 13.

The function

$$\frac{nS_u(n)}{\beta_u u_{*0}^2} = \frac{C_u f/f_{mu}}{[1 + 1.5(f/f_{mu})^{r_u}]^{5/3r_u}} \tag{21}$$

was selected to represent the longitudinal spectrum, where C_u and r_u are positive constants determined by a least-squares analysis. For sufficiently small values of f, $nS_u(n)/\beta_u u_{*0}^2$ asymptotically behaves like f/f_{mu} which is the correct behavior for a one-dimensional spectrum. At large values of f, $nS_u(n)/\beta_u u_{*0}^2$ asymptotically behaves like $(f/f_{mu})^{-2/3}$ consistent with the concept of the inertial subrange. The maximum value of (21) occurs at $f = f_{mu}$. Various authors have suggested formulas like (21) to represent the longitudinal spectrum. However, most of the representations have only one adjustable parameter available, while (21) has two: C_u and r_u. In this respect, (21) seems to be superior. Upon setting $r_u = \frac{5}{3}$, we obtain the form of the longitudinal spectrum suggested by Panofsky[9] to represent the strong wind spectra of Davenport.[16] von Kármán's longitudinal spectrum[17] can be obtained by setting $r_u = 2$. A least-squares analysis of the longitudinal data in Fig. 13 revealed that $C_u = 6.198$ and $r_u = 0.845$.

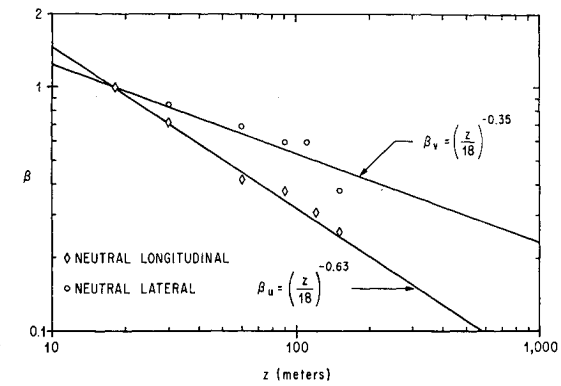

Fig. 12 The vertical distribution of the collapsing factors β_u and β_v for neutral stability conditions.

Lateral Spectrum

The lateral spectra S_v can be collapsed with a procedure like the one used for the longitudinal spectra. However, to determine an analytical expression for the lateral spectrum, special attention must be paid to the inertial subrange to guarantee that $S_u/S_v = \frac{3}{4}$ (see Ref. 18). This requirement is derived from the mass continuity equation for incompressible flow, subject to the condition that the eddies are isotropic in the inertial subrange. The experimental values of f_{mv} and β_v are given in Figs. 11 and 12. The function

$$\frac{nS_v(n)}{\beta_v u_{*0}^2} = \frac{C_v(f/f_{mv})}{[1 + 1.5(f/f_{mv})^{r_v}]^{5/3r_v}} \tag{22}$$

was used to represent the scaled spectra, where C_v and r_v are positive constants. This function behaves like the one chosen for the longitudinal spectrum.

For sufficiently large values of f, the asymptotic behavior of the ratio between (21) and (22) is given by

$$S_u/S_v \sim (C_u/C_v)\,(\beta_u/\beta_v)(f_{mu}/f_{mv})^{2/3}\,\tfrac{3}{2}^{(5/3)}\left(\frac{1}{r_v} - \frac{1}{r_u}\right) \tag{23}$$

In the inertial subrange we must have $S_u/S_v = \frac{3}{4}$, so that upon substituting this ratio into (23) we obtain a relationship that can be used as a constraint in the determination of values of C_v and r_v and functions to represent β_v and f_{mv}. The values $C_v = 3.954$ and $r_v = 0.781$, the functions

$$f_{mv} = 0.1(z/18)^{0.58} \tag{24}$$

and

$$\beta_v = (z/18)^{-0.35} \tag{25}$$

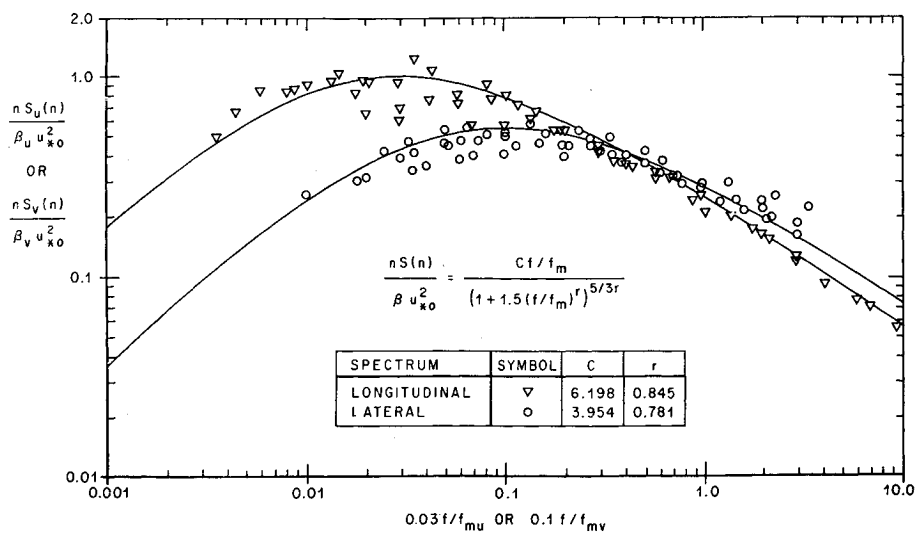

Fig. 13 Dimensionless logarithmic longitudinal and lateral spectra as functions of $0.03\,f/f_{mu}$ and $0.1\,f/f_{mv}$ for neutral stability conditions.

and the longitudinal parameters will satisfy condition (23) and simultaneously give a good fit to the data (z is in meters). The collapsed lateral spectra and the functions given by (21) and (22) are shown in Fig. 13.

Engineering Application

To apply the longitudinal and lateral spectra of turbulence to engineering problems, we first select the design peak-wind speed u_{18} for a prescribed level of risk based on the period of time the vehicle will be exposed to the natural environment. At Marshall Space Flight Center, the peak-wind profile is established by selecting the 99.87 percentile value of k consistent with this value of u_{18}. The mean-wind profile is obtained by dividing the peak wind profile by the gust factor associated with an averaging time equal to 10 min. The friction velocity u_{*0} is calculated with (10) for neutral wind conditions [$Ri = 0, \psi(0) = 0$]. Once the mean-wind speed profile and the friction velocity are known, the longitudinal and lateral spectra are completely specified.

At this point, the calculations of the turbulent loads would be performed with methods like the ones used by Wood and Berry[19] and Reed.[20]

Conclusions

Development of space vehicle wind loads design criteria is not simple, but is rather a complicated procedure requiring the designer and the atmospheric scientist to work as a team. The engineer must specify the risk he is willing to accept, while the atmospheric scientist must produce a wind model from which it is possible to determine the appropriate forcing functions for that accepted risk. The model presented here for the Kennedy Space Center, serves this purpose in that risk values can be applied to the occurrence of peak-wind speeds at a reference height for a given period of exposure, and if these design peak-wind speeds occur, an upper bound risk value of structural failure can be estimated from statistical information about the wind profile shape (k). By applying gust factors for an appropriate averaging period, a peak-wind speed environment can be partitioned into mean wind and turbulence environments.

References

[1] Smith, O. E., Falls, L. W., and Brown, S. C., "A Statistical Analysis of Winds for Aerospace Vehicle Design, Mission Planning, and Operations," *Research Achievements Review*, Vol. II, Rept. 10, 1967; also TM X-53706, NASA.

[2] Fisher, R. A., *Contributions to Mathematical Statistics*, Wiley, New York, 1950, pp. 15.179a–15.190.

[3] Gumbel, E. J., *Statistics of Extremes*, Columbia Univ. Press, New York, 1958.

[4] Thom, H. C. S., "Distribution of Extreme Winds in the United States," *Journal of the Structural Division Proceedings of the American Society of Civil Engineers*, Vol. 86, April 1960, pp. 11–24.

[5] Kaufman, J. W. and Keene, L. F., "NASA's 150-Meter Meterological Tower Located at Cape Kennedy, Florida," TM X-53259, May 1965, NASA.

[6] Fichtl, G. H., "Characteristics of Turbulence Observed at the NASA 150-m Meteorological Tower," *Journal Applied Meteorology*, Vol. 7, 1968, pp. 838–844.

[7] Fichtl, G. H. and McVehil, G. E., "Longitudinal and Lateral Spectra of Turbulence in the Atmospheric Boundary Layer," presented at the AGARD Specialists' Meeting on The Aerodynamics of Atmosphereic Shear Flows, Munich, Sept. 15–17, 1969.

[8] Monin, A. S., "On the Similarity of Turbulence in the Presence of a Mean Vertical Temperature Gradient," *Journal Geophysical Research*, Vol. 64, 1959.

[9] Lumley, J. L. and Panofsky, H. A., *The Structure of Atmospheric Turbulence*, Wiley, New York, 1964.

[10] Panofsky, H. A., Blackadar, A. K., and McVehil, G. E., "The Diabatic Wind Profile," *Quarterly Journal of The Royal Meteorological Society*, Vol. 86, 1960, pp. 390–398.

[11] Davenport, A. G., "The Relationship of Wind Structure to Wind Loading," presented at the Meeting on Ground Wind Load Problems in Relation to Launch Vehicles, NASA Langley Research Center, June 7–8, 1966.

[12] Blackman, R. B. and Tukey, J. W., *The Measurement of Power Spectra*, Dover, New York, 1958.

[13] Pasquill, F., *Atmospheric Diffusion*, Van Nostrand, New York, 1962.

[14] Berman, S., "Estimating the Longitudinal Wind Spectrum Near the Ground," *Quarterly Journal of the Royal Meteorological Society*, 91, 1965, pp. 302–317.

[15] Busch, N. E. and Panofsky, H. A., "Recent Spectra of Atmospheric Turbulence," *Quarterly Journal of the Royal Meteorological Society*, Vol. 94, 1968, pp. 132–148.

[16] Davenport, A. G., "The Spectrum of Horizontal Gustiness Near the Ground in High Winds," *Quarterly Journal of the Royal Meterological Society*, Vol. 87, 1961, pp. 194–211.

[17] von Kármán, T., "Progress in the Statistical Theory of Turbulence," *Turbulence-Classic Papers on Statistical Theory*, Interscience, New York, 1961, pp. 162–174.

[18] Batchelor, G. K., *The Theory of Homogeneous Turbulence*, Cambridge Univ. Press, New York, 1953.

[19] Wood, J. D. and Berry, J. G., "Random Excitation of Missiles Due to Winds," *Proceedings of the National Symposium on Winds for Aerospace Vehicle Design*, Vol. 1; also AFCRL-62-273(I), USAF Geophysics Res. Dir. A. F. Surveys in Geophysics, No. 140, Vol. 1, March 1962, pp. 125–138.

[20] Reed, W. H., III, "Models for Obtaining Effects of Ground Winds on Space Vehicles Erected on the Launch Pad," presented at the Conference on the Role of Simulation in Space Technology, Virginia Polytechnic Institute, Blacksburg, Va., Aug. 17–21, 1964.